Separation and Purification Technology 354 (2025) 128828

Contents lists available at ScienceDirect

Separation and Purification Technology

journal homepage: www.elsevier.com/locate/seppur

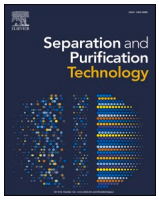

Towards an electrochemically-based circular economy: Electro-refinery for valorizing phenolic wastewater

Raíra S. S. Castro [a,b,d], Géssica O. S. Santos [c], Marcos Roberto V. Lanza [c], Giancarlo R. Salazar-Banda [a,b], Katlin I. B. Eguiluz [a,b], Cristina Sáez [d], Manuel Andrés Rodrigo [d,*]

[a] Electrochemistry and Nanotechnology Laboratory, Institute of Technology and Research (ITP), 49032-490, Aracaju-SE, Brazil
[b] Graduate Program in Process Engineering (PEP), Universidade Tiradentes, 49032-490, Aracaju-SE, Brazil
[c] University of São Paulo, São Carlos, Brazil
[d] Chemical Engineering Department, University of Castilla-La Mancha, Ciudad Real, Spain

ARTICLE INFO

Keywords:
Electrorefinery
Anionic membrane
Carboxylates
Highly added value products

ABSTRACT

This study introduces an innovative approach to wastewater treatment that combines two electrochemical technologies: electrolysis and electrochemical separation facilitated by anionic exchange membranes. This integrated technology converts pollutants into carboxylates, which are valuable intermediates for further electrosynthesis and fuel production. The efficacy of this approach was demonstrated using synthetic wastewater containing phenol as a model pollutant, chosen for its well-documented characteristics that enable comparative analysis with previous studies. The treatment process utilized mixed metal oxides (MMO) anodes with a composition of $Ti/(RuO_2)_{0.8}(Sb_2O_4)_{0.2}$ and a boron-doped diamond (BDD) anode. The investigation was structured to evaluate each component of the treatment system individually before examining their collective performance. Through a series of case studies, the research not only confirmed the feasibility of this innovative technology but also highlighted the need for further study on the optimization of operational parameters and electrode materials. Comparative analysis revealed that MMO anodes outperformed BDD anodes, achieving maximum carboxylate transport rates of 138.7 mmol $m^{-2}h^{-1}$. The efficiency of carboxylate separation from the solution where they were generated reached up to 54.6 mmol kWh^{-1}, while the maximum overall production efficiency was 8.77 mmol kWh^{-1}. The study further determined that current density significantly affects both the production rate and the extent of mineralization, identifying optimal densities of 100 mA cm^{-2} and 30 mA cm^{-2} for the electrolyzer and electroseparator units, respectively. This work provides valuable insights for the optimization of this promising wastewater treatment technology, with potential applications in various industries.

1. Introduction

The development of more sustainable technologies, even in the field of environmental remediation, is a real necessity for current society, given the lack of resources and energy required to supply a planet with a fast-growing population efficiently [1–5].

The paradigm of treatment technologies primarily focused on pollutant mineralization is nearing its conclusion. Carbon dioxide, a byproduct of these processes, not only lacks economic value but also significantly contributes to global warming. In contrast, the current emphasis is on technologies that convert pollutants into valuable resources [6]. In fact, the concept of waste recovery has undergone significant evolution over the recent years, being subjected to extensive research trying to demonstrate an increased capacity for the practical realization of circular economy principles [7]. Consequently, industrial processes, including those for environmental remediation, are increasingly aimed at repurposing or recycling waste into valuable products or energy, aligning with the evolving priorities of sustainability and resource efficiency.

Although there are several approaches, an exciting possibility is the transformation of complex organic pollutants into carboxylates by electrochemically assisted oxidative processes and in their separation using membrane-assisted electrodialysis technology. This concept has been introduced elsewhere [6,8], but up to now, it has not been proved as a whole but only as different parts that can be integrated.

Electrochemical technology not only offers potential applications but

* Corresponding author.
E-mail address: manuel.rodrigo@uclm.es (M.A. Rodrigo).

https://doi.org/10.1016/j.seppur.2024.128828
Received 27 April 2024; Received in revised form 1 July 2024; Accepted 14 July 2024
Available online 15 July 2024

also presents a compelling case for its adoption in environmental remediation efforts [9,10]. Its established use in metal recovery through electrodeposition and purification via inorganic electrorefining has been well-documented for decades. More recently, a novel concept has emerged, broadening the scope of electrochemical applications to include the recovery of organic pollutants. This innovative approach envisions converting these pollutants into building blocks for product synthesis or fuel production [11].

Various strategies have been explored in this context, among which the electrochemical conversion of complex organic pollutants into carboxylates presents a noteworthy approach. This process uses oxidative electrochemical reactions, coupled with membrane-assisted electrodialysis (ED), to effectively separate the resulting compounds. Although this concept has been previously suggested in the literature, to the knowledge of the authors its implementation has only been proven in separate stages and not in the same integrated process [6,8]. The ongoing advancements in membrane technology, process integration, and optimization further amplify the significance and potential applicability of the strategy proposed, promising more efficient, cost-effective, and environmentally benign solutions for a wide range of waste treatment applications [12,13]. Of special interest is the progress in the separation and purification of carboxylates, where Mandal et al. 2020 reported a selective transport of carboxylic acids (acetic, malic, and citric acid) from the ternary mixture through ED using different anion exchange membranes [14] and Hernandez et al. 2021 demonstrated the feasibility of using conventional monopolar ion exchange membranes for the efficient separation of short- and medium-chain carboxylic acids (acetic, butyric and caproic acids) from a synthetic fermentation broth with a total recovery efficiency of 60 ± 3 % (mol mol^{-1}) [15]. On the other hand, important progress in engineering aspects and in scaling up have been highlighted in some recent review papers [16,17]. To date, the approach aimed to be evaluated in this work has been demonstrated in separate components rather than as an integrated process, indicating a need for further research to realize its full potential.

In the context of this research, our study aims to demonstrate the effective generation and recovery of value-added products derived from the electrolysis of phenol. This approach represents a relatively unexplored avenue within the field of electrochemically assisted wastewater treatment [6]. For the past three decades, phenol has served as a benchmark pollutant in numerous studies assessing the efficacy of various oxidation technologies, including electrolysis. Its aromatic nature and high solubility drive its choice as a subject of study in water, which has made its oxidation pathways and the intermediates it produces well-documented [18–23]. The extensive body of research on phenol and its oxidation intermediates underpins its selection for this study.

2. Materials & methods

2.1. Electrolysis cell

This single-compartment cell was equipped with a mixed metal oxide (MMO) anode, consisting of a coating of antimony and ruthenium oxides supported on a titanium plate with a composition of Ti/$(RuO_2)_{0.8}(Sb_2O_4)_{0.2}$, and a stainless-steel (AISI 314) cathode, with both electrodes measuring 3.0 × 3.0 cm^2. The MMO electrodes were synthesized following a methodology detailed elsewhere [24]. For certain experiments, the MMO electrode was replaced with a boron-doped diamond electrode (BDD) purchased from Neocoat, France. This electrode comprised a BDD layer, characterized by a sp^3/sp^2 ratio of 150 and a boron content of 500 ppm, supported on a p-type silicon (p-Si) plate with a thickness of 2 mm and a resistivity of 100 mΩ cm. The electrochemical cell was fabricated in our laboratory using 3D printing technology, specifically stereolithography, adhering to a process previously outlined in the literature [25]. The electrodes were integrated into a resin frame and shielded by a gas mask, which confined the active surface area to a circular section with a 3.0 cm diameter. The gap between electrodes in the cell comprises a single compartment, mechanically engineered to facilitate high turbulence, enhancing the efficiency of the electrolysis process. Further elaboration and visual details of this configuration are provided in Fig. 1.

2.2. Electroseparation cell

This cell is a double-compartment cell made with the same concept pieces used in the electrolysis cell, and it was equipped with the same type of MMO (Ti/$(RuO_2)_{0.8}(Sb_2O_4)_{0.2}$) anode and stainless steel (AISI 314) cathode than the electrolysis cell (sizing 3.0 × 3.0 cm^2). The main difference between the two cells lies in the cell's structure, where the electroseparation unit includes a duplicated frame design with a membrane interposed to segregate the compartments. The selected membrane was a RALEX® AMH-PES type, measuring 860 mm in roll length, purchased from MemBrain s.r.o. (Czech Republic). Similar to the electrolysis experiments, in particular tests within the electroseparation context, the MMO anode was replaced by a BDD electrode.

2.3. Electrorefinery concept setup

Both electrochemical cells described above were integrated into a hydraulic circuit, as illustrated in part 2 of Fig. 1. This setup includes two storage tanks, each with a capacity of 100 cm^3. Tank 1 contains the wastewater subject to electrochemical treatment, while Tank 2 holds a solution that becomes enriched with carboxylates as the process progresses. The wastewater consisted of a synthetic solution composed of 3.0 g L^{-1} NaOH – 3.0 g L^{-1} Na_2SO_4 and 300 mg L^{-1} phenol. The system employs three pumps (P Selecta, Percom N-M) to manage fluid movement: two pumps connect the electrolysis cell and the cathodic compartment of the electroseparation cell with Tank 1, facilitating the introduction of wastewater into these units. The third pump is responsible for circulating the liquid between Tank 2 and the anodic compartment of the electroseparation cell. The flow rate across the system is consistently maintained at 100 cm^3 min^{-1}.

2.4. Experimental methodology

The phenol removal efficiency was evaluated by employing high-performance liquid chromatography (HPLC) with a Shimadzu − UFLC 20 system, which was connected to a UV detector. The chromatographic separation was achieved using a Phenomenex reversed-phase C8 column, which measured 150 × 4.6 mm and had a particle size of 5 μm. The mobile phase comprised a 70:30 v/v mixture of acetonitrile and 10% formic acid solution, delivered at a flow rate of 0.8 mL min^{-1} at a temperature of 40 °C. Phenol detection was performed at a wavelength of 280 nm, with an injection volume set to 20 μL and a retention time recorded at 5.8 min. The same HPLC Shimadzu − UFLC 20 system equipped with a UV detector was employed to quantify carboxylates. Separation was facilitated by a Hiplex H reversed-phase column with dimensions of 300 × 7.7 mm. The mobile phase in this analysis was 0.1 M sulfuric acid, flowing at 0.6 mL min^{-1} at a temperature setting of 60 °C.

3. Results & discussion

3.1. Evaluation of carboxylic acid recovery in the electroseparation cell

The potential for carboxylic acid separation using the electroseparation cell was investigated through various experiments using synthetic solutions. These solutions contained the main carboxylate anions predicted from the degradation of phenolic wastes, as reported in existing literature [26–30].

Initially, the performance of the membrane, intended for integration

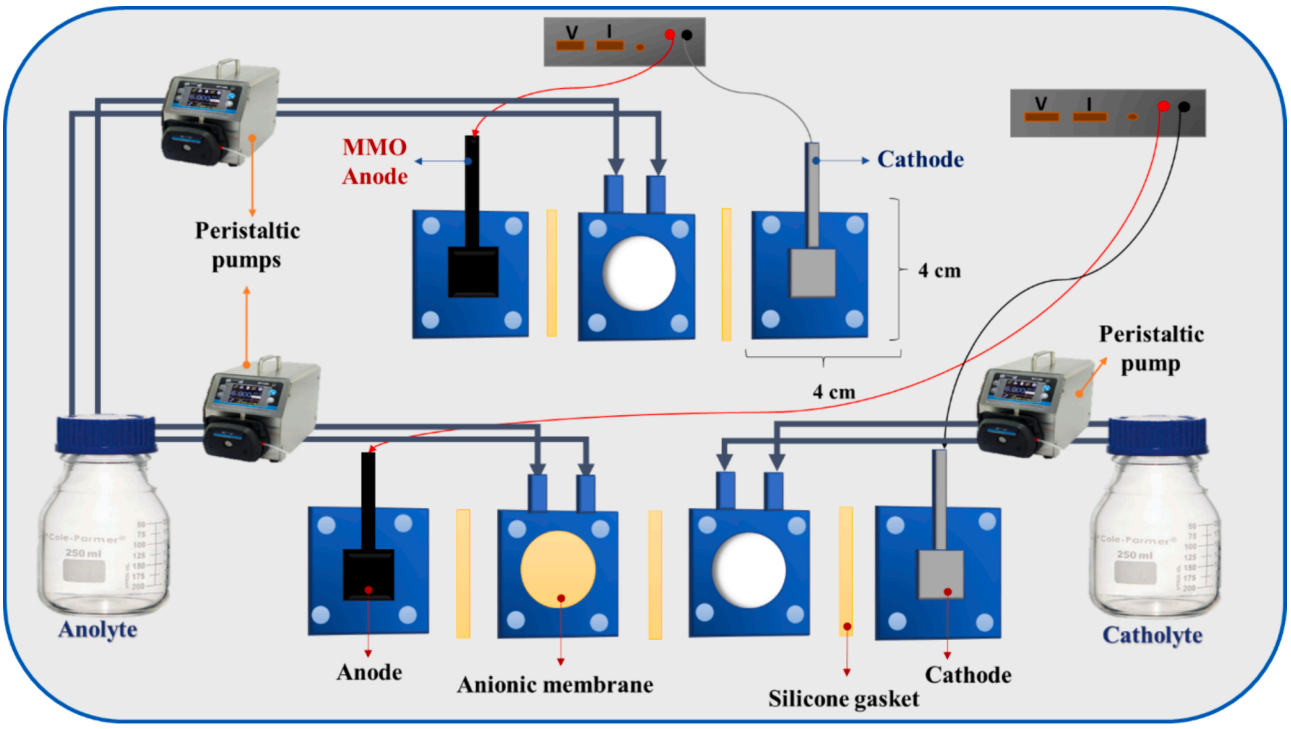

Fig. 1. Experimental setup for the electro-refinery concept.

into the electroseparation cell, was evaluated in the presence of carboxylate solutions. Results are shown in Fig. 2 for the oxalate anion, revealing the membrane's behavior. Fig. 2a demonstrates that immersing the anionic membrane in a solution with a concentration of 300 ppm of oxalate results in no significant change in the oxalate concentration after about two days. This observation suggests minimal to no irreversible interaction between the anion and the membrane, as evidenced by the lack of alteration in both the composition of the membrane and the concentration of the solution during the tested period.

Moreover, it was considered essential to check the significance of the transport by diffusion through the membrane (Fig. 2b). Results indicate that diffusion does occur even in the absence of an applied electric field. This was determined by monitoring concentration changes in a dual-compartment cell, where one compartment contained a solution with the target carboxylate, and the other held the same solution minus the

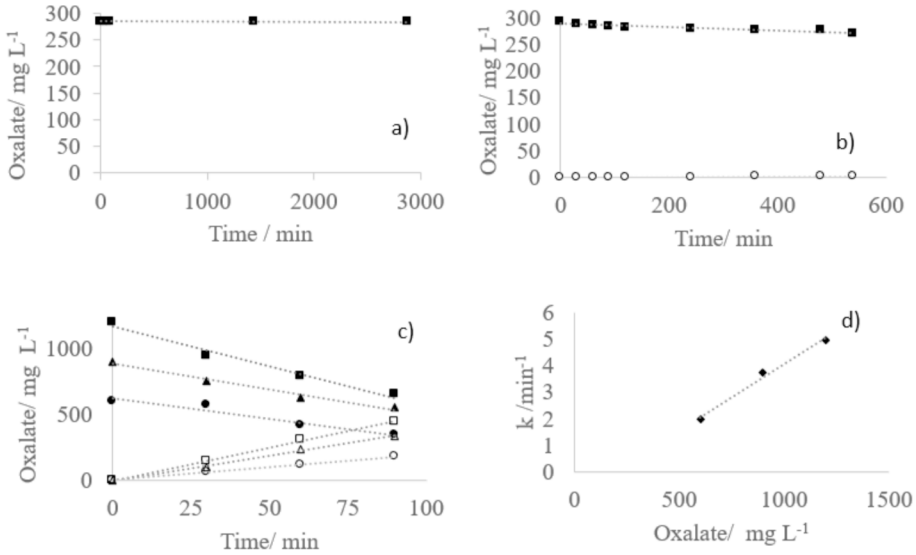

Fig. 2. Interaction of the membrane with oxalate solutions containing 300 mg L^{-1} of oxalate (3.33 mM), 3.0 g L^{-1} NaOH, and 3.0 g L^{-1} Na_2SO_4. a) Depicts the changes in the concentration of oxalate in the solution when a piece of membrane (3.0 × 3.0 cm^2) is submerged into the oxalate solution (■), b) Illustrates the diffusion-driven transport across the membrane in the absence of an electric field (■ compartment with 300 mg L^{-1} of oxalate, 3.0 g L^{-1} NaOH and 3.0 g L^{-1} Na_2SO_4 solution, ● compartment with 3.0 g L^{-1} NaOH and 3.0 g L^{-1} Na_2SO_4 solution), c) Transport in the cell under the application of electric field (current density applied 30 mA cm^{-2}) in solutions containing 3.0 g L^{-1}NaOH and 3.0 g L^{-1} Na_2SO_4 and 600, 900 and 1200 mg L^{-1} of oxalate. Cathode solution (▲ 600 mg L^{-1}, ◆900 mg L^{-1}, ●1200 mg L^{-1}) anode solution (Δ 600 mg L^{-1}, □ 900 mg L^{-1}, ○ 1200 mg L^{-1}). d) Carboxylate transport rate calculated from the mass balance at 30 mA cm^{-2}. The setup used a RALEX® AMH-PES anionic membrane, a $Ti/(RuO_2)_{0.8}(Sb_2O_4)_{0.2}$ anode, and a stainless steel (AISI 314) cathode, with both anolyte and catholyte volumes set at 100 cm^3.

carboxylate. Despite this, the extent of diffusion was found to be minimal, with less than 2% of the oxalate migrating from one compartment to another over a nine-hour period.

In contrast, the dynamics of transport under an applied electric field, shown in Fig. 2c, revealed a direct correlation with concentration, thereby suggesting that concentration is a limiting factor in the overall transport process. This is further corroborated by a mass balance-derived calculation of the transport rate, which exhibited a linear relationship with increasing concentration, as depicted in Fig. 2d.

Following the verification of carboxylate transport feasibility within the cell, a comprehensive series of experiments were conducted to characterize this transport phenomenon deeply in the electroseparation cell. Key findings from these experiments are presented in Fig. 3. These experiments aimed to quantify the transport of the most significant carboxylates generated during phenol degradation from the cathode to the anode compartment across varying current densities. Conducted under galvanostatic conditions, each test maintained a constant operational current density, observing that the operational cell voltage remained relatively stable throughout (with a standard deviation less than 0.35% of the mean value), which, as anticipated, showed an increase alongside the current density (as depicted in Fig. 3a).

In all instances, a linear rise in carboxylate concentration within the anodic compartment was noted over time. The oxidation of carboxylates, as well as their transport rates, were deduced from mass balance calculations. Fig. 3b illustrates that the oxidation rate of different carboxylates varies significantly with the applied current density, but this parameter does not affect all carboxylates in the same way. For instance, formate showed no degradation throughout the experiment, whereas acetate primarily underwent oxidation at lower current densities but not higher ones. In contrast, oxalate experienced the most substantial changes, indicating differential reactivity and transport behavior under varying electrochemical conditions.

Fig. 3c details the transport rates achieved during tests conducted at various current densities, lasting three hours each. During these intervals, a consistent linear increase in carboxylate concentration within the anodic compartment was noted, allowing for the calculation of transport rate values. The data reveal that the transport rate is influenced not only by the applied current density but also by the specific carboxylate in question. Among the carboxylates tested, oxalate demonstrated the highest transport rate, followed by maleate, acetate, and formate. Furthermore, it was observed that operating at current densities above 30 mA cm^{-2} does not result in significant improvements in transport efficiency, indicating a limitation in the transport rate beyond this point. This insight is crucial for determining the optimal operational current density for the process, as higher current densities lead to increased cell voltage and, consequently, higher energy consumption. This phenomenon is further observed in Fig. 3d, which illustrates that the efficiency of carboxylate separation depends on both the applied current density and the type of carboxylic acid being transported, following the order of maleate < acetate < formate < oxalate in increasing efficiency. Two factors are proposed to explain these variations: ionic conductivity and the size of the anion. Specifically, ionic conductivities are found to increase in the order of acetate (40.9 10^{-4} m^2 S mol^{-1}) < formate (54.6 10^{-4} m^2 S mol^{-1}) < maleate (61.9 10^{-4} m^2 S mol^{-1}) < oxalate (74.11 10^{-4} m^2 S mol^{-1}). This sequence suggests an anomalous behavior for acetate, potentially related to its molecular size, providing a nuanced understanding of the factors influencing carboxylate transport efficiency.

3.2. Employing the electroseparation cell to valorize phenol electrolysis products

Fig. 4 shows the changes in concentrations of different species within the treated wastewater as phenol undergoes degradation in the electrolysis cell under galvanostatic conditions. Consistent with existing literature [26,31,32], aromatic compounds (mainly hydroquinone and benzoquinone) and various carboxylates (mainly oxalate) are sequentially produced, prior to their complete mineralization into carbon dioxide, the latter representing the terminal phase of the treatment if electrolysis continues for a sufficient duration. However, the focus of this study was not on achieving mineralization. The conditions (100 mA cm^{-2}) and the anode material (mixed metal oxide) were explicitly chosen to maximize phenol conversion to the desired by-products (carboxylates) [33–36]. This strategic choice is evident in Fig. 4a, where the time-dependent concentration profile of aromatic intermediates (including benzoquinone and hydroquinone) exhibits a

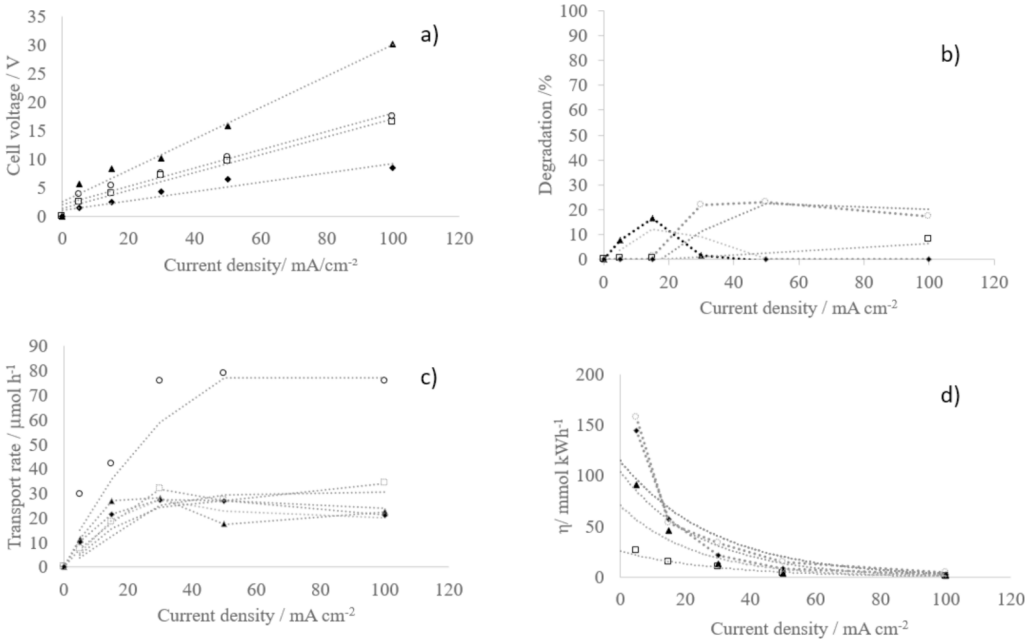

Fig. 3. Impact of current density on carboxylate transport in synthetic solutions. The figure presents the transport behaviors of various carboxylates (oxalate ○, acetate ▲, maleate □, and formate ◆) under different current densities applied for 3 h. (a) Displays the cell voltage. (b) Illustrates the total degradation of each carboxylate species after three hours of current application. (c) Displays the transport rates of carboxylates. (d) Evaluates the efficiency of carboxylate transport.

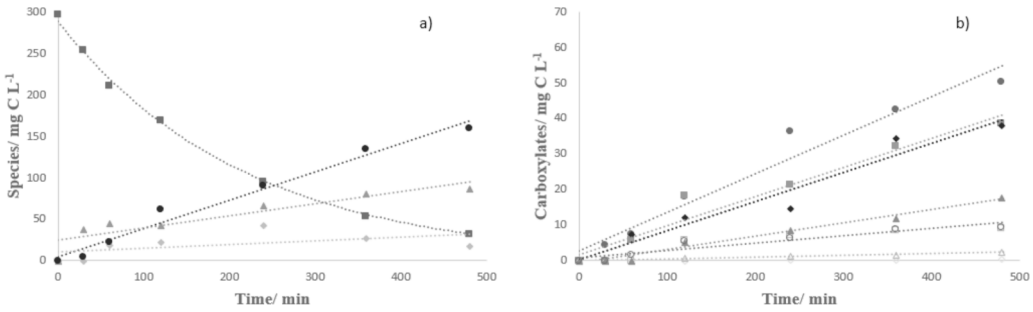

Fig. 4. Variation in species concentrations in wastewater treated via electrolysis: The figure depicts the concentration changes of various species within wastewater subjected to electrolysis at 100 mA cm^{-2} using an MMO anode. The initial solution consisted of 300 mg L^{-1} phenol, 3.0 g L^{-1} NaOH, and 3.0 g L^{-1} Na_2SO_4. (a) Overall speciation includes CO_2 ▲, Phenol ■, Aromatic ◆, and Carboxylates ●. (b) Breakdown of carboxylate speciation shows Acetate ▲, Malonate ■, Maleate ◆, Oxalate ●, Propanoate ○, Formate Δ, Oxamate □, and Succinate ◊.

typical pattern for an intermediate compound. In contrast, the production of carboxylates shows a continuous increase over time. This pattern underscores the targeted approach of the study to valorize the electrolysis products of phenol by diverting the pathway from complete mineralization to the generation of valuable carboxylate intermediates.

In the study of carboxylates (Fig. 4b), analysis of the samples obtained during the electrolysis identified up to eight carboxylate species, with oxalate, maleate, and malonate being predominant. This is the expected result, considering the known refractory character of oxalate and maleate, as compared with other carboxylates, facilitating their accumulation in the system (see systems 1 and 2 in Fig. 1). At this point, it is crucial to highlight that the conditions under which this electrolysis was performed markedly differ from those described in previous studies. The use of a strongly alkaline electrolyte sets this research apart from earlier work [18,20,22,23], as such conditions are generally less conducive to the oxidation of organic compounds. This is attributed to the reduced efficiency of potential oxidative mediators (like peroxosulfate and ozone produced at the anode or hydrogen peroxide produced at the cathode) in strongly alkaline environments, thereby diminishing their oxidative impact in the solution.

Furthermore, the prominent presence of malonate among the primary oxidation products warrants attention. This finding diverges from the bulk of phenol-related literature, which predominantly reports the generation of oxalate and maleate. This discrepancy may be explained by the unique electrolytic conditions employed in this study, which influence the efficiency of organic compound oxidation and the resultant spectrum of carboxylate species produced. For comparison purposes, Table 1 presents the most significant results in the literature for the formation of carboxylic acids through the oxidation of different organic compounds. As seen, regardless of the initial pollutant, the electrolytic process always results in the production of carboxylates (or their corresponding acids) in concentration that depends on the initial concentration of the pollutant but that are within the range obtained in this work during the oxidation of phenol.

The final solution resulting from the electrolytic degradation of phenol-contaminated wastewater was divided into six aliquots. Each aliquot was subjected to a distinct treatment process in the electroseparation unit, differentiated by the application of varying operational current densities (15, 30, and 60 mA cm^{-2}). In addition, separation efficacy was evaluated using either an MMO or a BDD anode within the electroseparation cell. The changes in the concentrations of the different carboxylates accumulated in tank 2 were monitored, and a linear increase was observed over time. This data facilitated the calculation of both the transport rate and efficiency for these tests. The results are summarized in Fig. 5.

The selection of anodic material in the electroseparation cell significantly influences the process, with observed differences between the use of MMO and BDD anodes. These differences refer to the mineralization of carboxylates within the cell, suggesting a preference for the MMO anode over the BDD anode for this stage of separation. The MMO anode facilitates milder operating conditions in the anodic chamber, thereby minimizing further mineralization of carboxylates during separation. Regarding operational current density, the data indicate an enhancement in carboxylate transport when the current density increases from 15 to 30 mA cm^{-2}. However, no significant improvement is observed between 30 and 60 mA cm^{-2}. This information agrees with the evidence provided in Fig. 3, which shows that beyond a current density of 30 mA cm^{-2}, there is no further enhancement in the electroseparation unit's performance. Additionally, the impact of current density on energy consumption is noteworthy, as increased current density leads to higher operation cell voltages and, consequently, elevated energy costs associated with carboxylate separation. This outcome highlights a

Table 1
Examples of systems that promote the formation of carboxylic acids through the oxidation of organic compounds.

Anode	Organic contaminant	Experimental conditions	Carboxylic acids	Ref.
BDD, SS	Dye Acid Green 25	V=0.1 L of AG25 solution (0.07 mM–0.60 mM), 50 mM (SO_4^{2-}, ClO_4^-, Cl^-), j = 50, 75, 100, 125 mA cm^{-2}, t = 360 min	j = 100 mA cm^{-2} Oxalic = 1.17 mg L^{-1} Oxamic = 5.34 mg L^{-1} Tartronic acid = 0.60 mg L^{-1}	[34]
Ti,BDD	Cashew-Nut Shell Liquid	V=0.25 L of the t-CNSL 1.0 mol L^{-1} NaOH, 60 mA cm^{-2}, j = 40, 70, 100 mA cm^{-2}, t = 240 min	j = 100 mA cm^{-2} Oxalic = 709.43 mg L^{-1} Acetic = 257.62 mg L^{-1} Fumaric = 0.19 mg L^{-1} Formic = 7.82 mg L^{-1}	[37]
Ti/ RuO_2–IrO_2-RhO_x	Phenol	500 mg L^{-1} phenol, 20 mM Na_2SO_4, j = 200 A m^{-2}, t = 540 min	Oxalic = 29.70 mg L^{-1} Malic = 48.27 mg L^{-1} Acetic = 67.85 mg L^{-1} Fumaric = 8.12 mg L^{-1} Malonic = 39.0 mg L^{-1} Formic = 18.41 mg L^{-1} Maleic = 34.83 mg L^{-1}	[38]
Ti_4O_7/Ti, BDD	Antipyretic 4-Aminophenazone (4-APHE)	0.23 L of 0.192 mM 4-APHE, 50 mM Na_2SO_4, 0.2 mM Fe^{2+}, $j = 1.25 - 10.41$ mA cm^{-2}, 10 or 25 mM of Cl^-, HCO_3^- or NO_3^-, t = 480 min	Ti_4O_7/Ti Oxalic = 0.036 mg L^{-1} Maleic = 95.20 mg L^{-1} Oxamic = 1.06 mg L^{-1} Malic = 96.53 mg L^{-1} Glycoxylic = 9.62 mg L^{-1} Acetic = 0.90 mg L^{-1} BDD Oxalic = 27.00 mg L^{-1} Maleic = 20.89 mg L^{-1} Oxamic = 12.46 mg L^{-1} Malic = 13.40 mg L^{-1} Glycoxylic = 17.02 mg L^{-1} Acetic = 1.50 mg L^{-1}	[39]
Ti/ $RuO_2.Sb_2O_4$	Phenol	V=100 ml 300 mg L^{-1} phenol, 3 g L^{-1} Na_2SO_4, 3 g L^{-1} NaOH, j = 100 mA cm^2, t = 360 min	Oxalic = 42.15 mg L^{-1} Acetic = 24.09 mg L^{-1} Propanoic = 8.88 mg L^{-1} Fumaric = 8.12 mg L^{-1} Malonic = 28.55 mg L^{-1} Formic = 1.61 mg L^{-1} Maleic = 33.54 mg L^{-1} Succinic = 0.42 mg L^{-1}	This Work

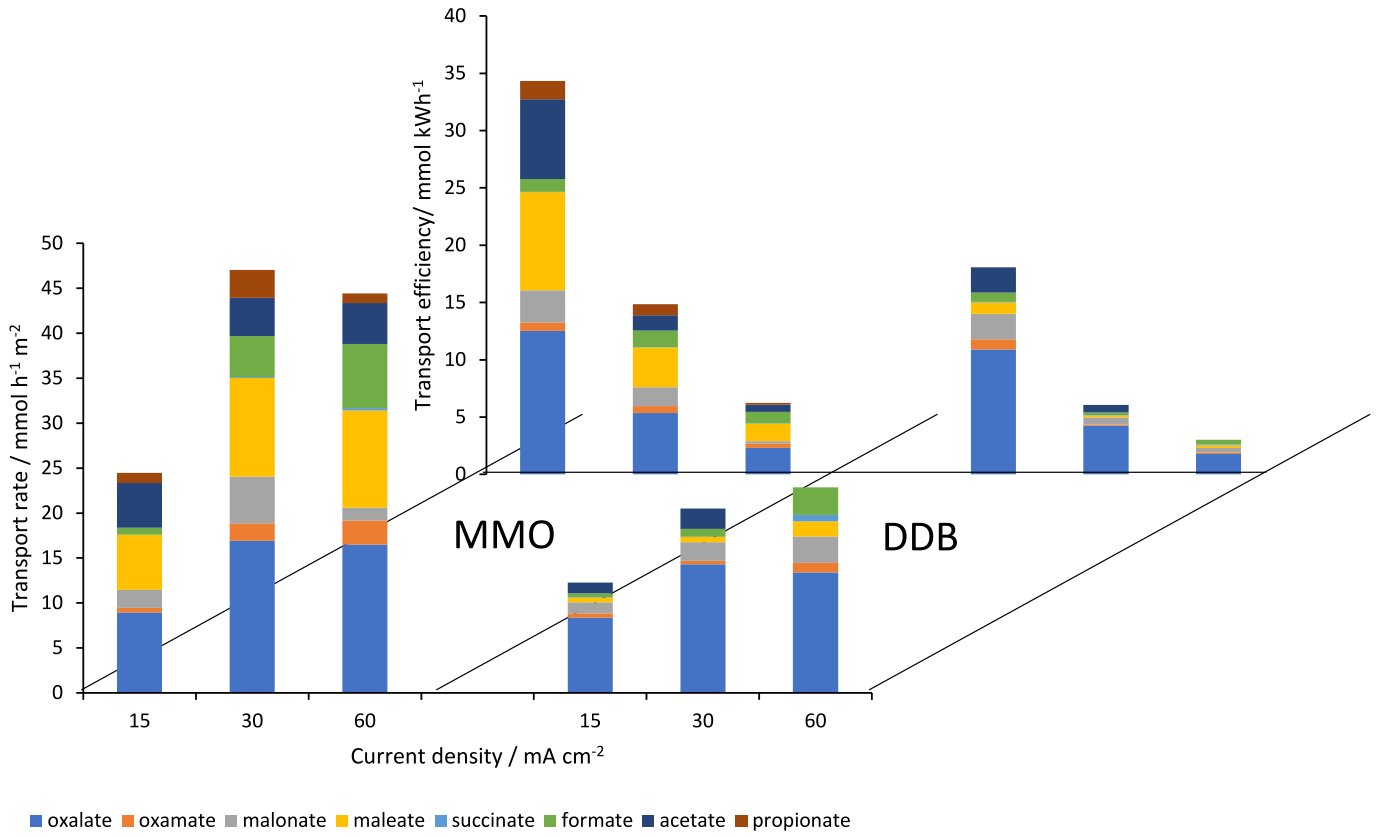

Fig. 5. Carboxylate Purification Performance. This figure presents a comparative analysis of carboxylate transport rates and purification efficiencies achieved with MMO and BDD electrodes. The analysis is based on the electrolyzer effluent, as described in the Experimental Section, highlighting the effectiveness of each electrode material in the electroseparation process.

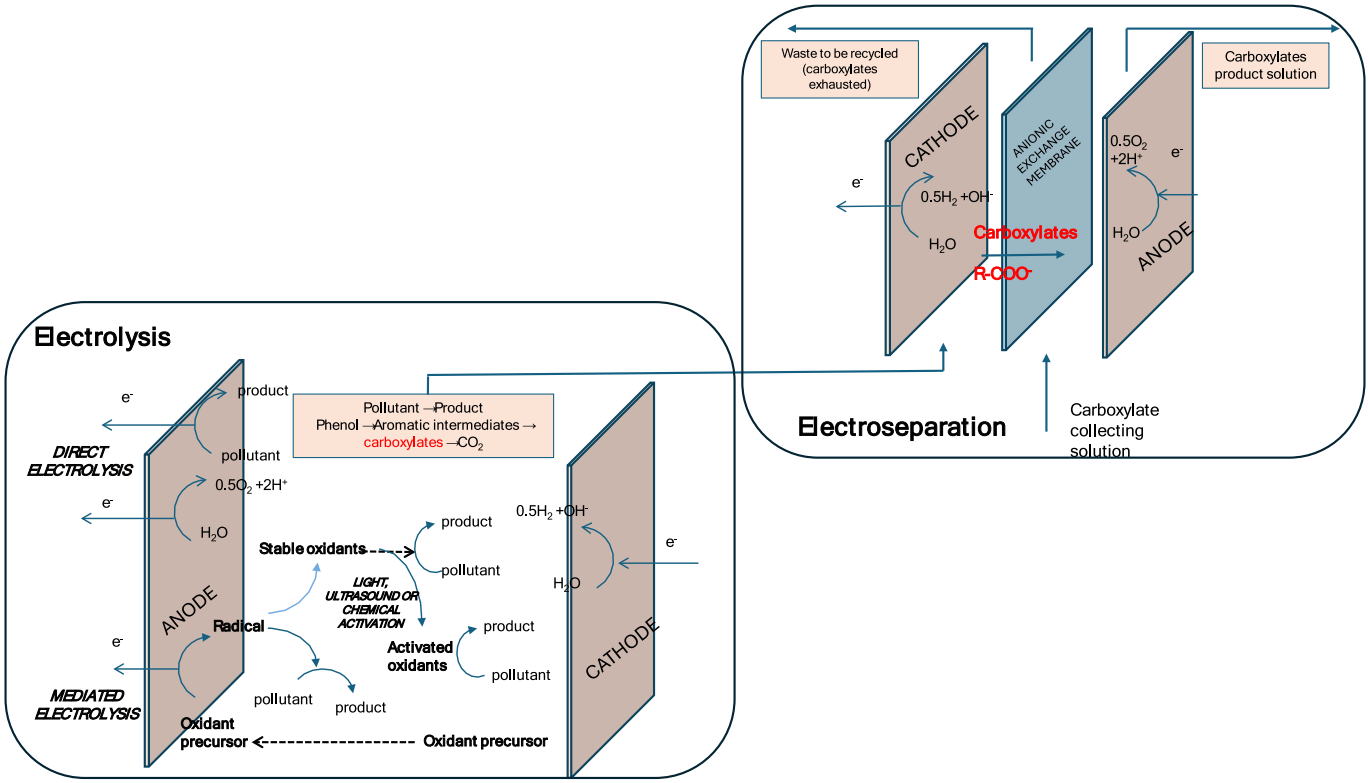

Fig. 6. Schematic concept model of the integrated electrochemically assisted refinery concept highlighting the main mechanisms involved.

diminished transport efficiency at higher current densities, necessitating a balance between transport rate and efficiency. Such a compromise must also consider the broader implications for capital expenditures (CAPEX), which tend to decrease with lower current densities, and operational expenses (OPEX), which increase with higher current densities. While preliminary, the insights derived from this study emphasize the need for comprehensive economic analysis in the optimization of electroseparation processes.

3.3. The integrated Electro-Refinery concept

This study has confirmed the feasibility of producing carboxylates in an electrolytic unit and the subsequent successful processing of the electrolysis effluent in an electroseparation unit. This process enables the efficient separation of carboxylates generated from the degradation of phenol. This section explores the potential for integrating these two processes within a single facility. To achieve this, both reactors were operated simultaneously, allowing for the direct recovery of carboxylates in a purified solution concurrently with the oxidation of phenol in synthetic wastewater, according to the procedure schematized in Fig. 6, where the main mechanisms are highlighted for both, the electrolytic and electrodialytic stages pointing out that main reaction expected, apart from water oxidation and reduction, are the electrochemical oxidation of phenol and intermediates either by direct or mediated processes.

Various test scenarios were executed to evaluate this integrated approach. An initial case study was conducted to identify optimal current densities for both units that would minimize the risk of mineralization. The MMO electrodes were considered beneficial, so the current densities were set to 50 mA cm^{-2} for the electrolytic unit and 15 mA cm^{-2} for the electroseparation unit. Fig. 7 illustrates the system's performance under these milder operational conditions for both cells.

Under the milder operational conditions implemented, the oxidation of phenol in the synthetic wastewater achieved less than a 50% conversion rate over an 8-hour treatment period. Despite this, the production and subsequent recovery of carboxylates into a distinct purified solution were successful, although the yield under these conservative conditions was not particularly high.

Given the modest recovery rates observed, exploring a second case study using higher current densities, specifically 100 mA cm^{-2} for the electrolysis unit and 30 mA cm^{-2} for the electroseparation unit, became imperative. The results of this adjusted approach are depicted in Fig. 8.

With the adjustment to higher current densities, the production of carboxylates has significantly improved in both tanks, stressing the importance of optimizing current densities as a critical factor in the successful application of this technology. Notably, higher concentrations

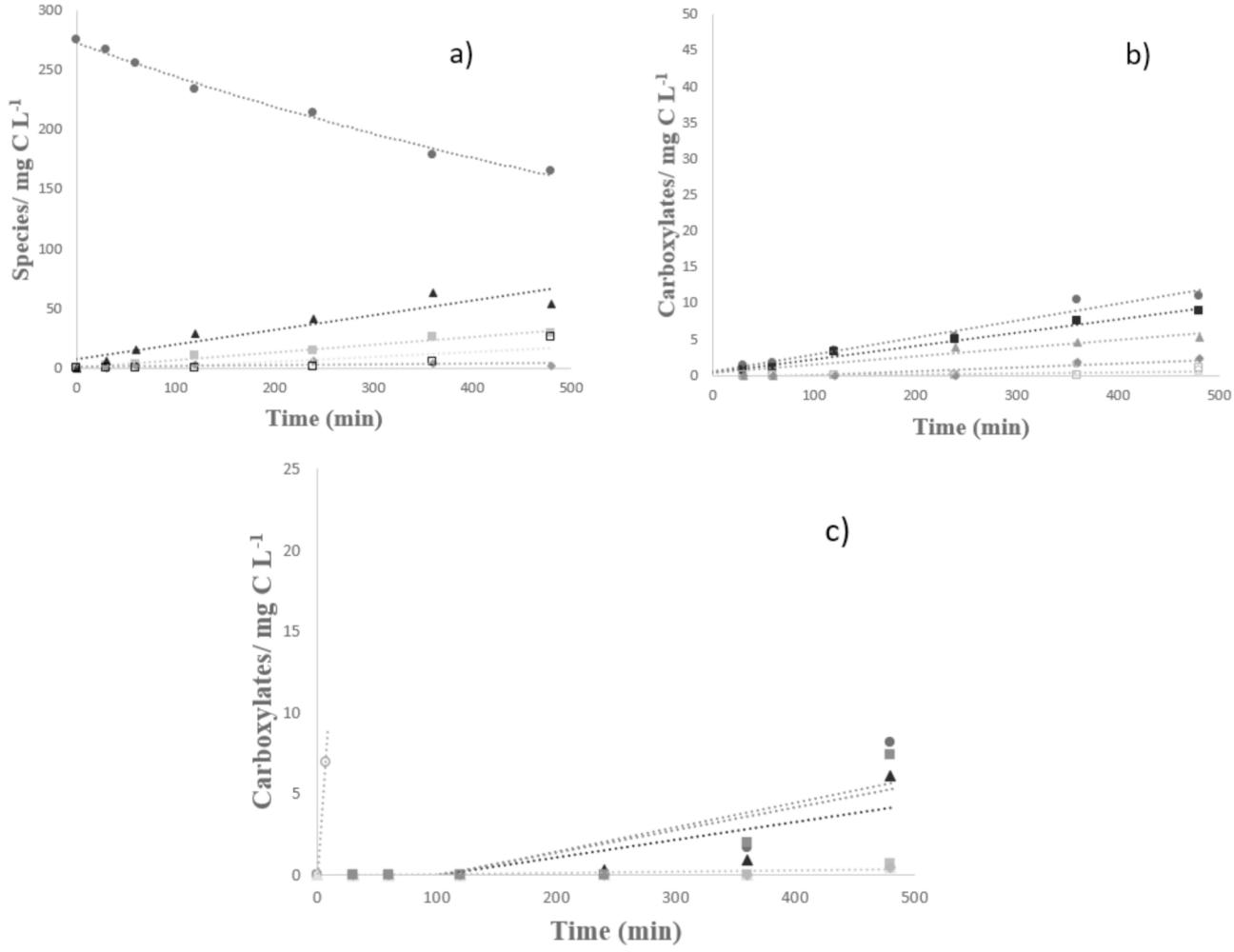

Fig. 7. Case study 1 in electro-refinery. Employing mild current densities for both electrolysis (50 $mAcm^{-2}$ with an MMO anode) and electroseparation units (15 $mAcm^{-2}$ with an MMO anode). a) Depicts overall species speciation in the treatment process: Phenol (●), carboxylates in tank 1 (■), carboxylates in tank 2 (□), Aromatics (◆), and CO_2 (▲). Graphics (b) and (c) detail the speciation of carboxylates in tanks 1 and 2, respectively, highlighting Malonate (▲), Maleate (■), Acetate (◆), Oxalate (●), Succinate (▬), Oxamate (○), and Formate (□). The wastewater tested contained 300 mg L^{-1} of phenol dissolved in a solution of 3.0 g/L NaOH and 3.0 g/L Na_2SO_4.

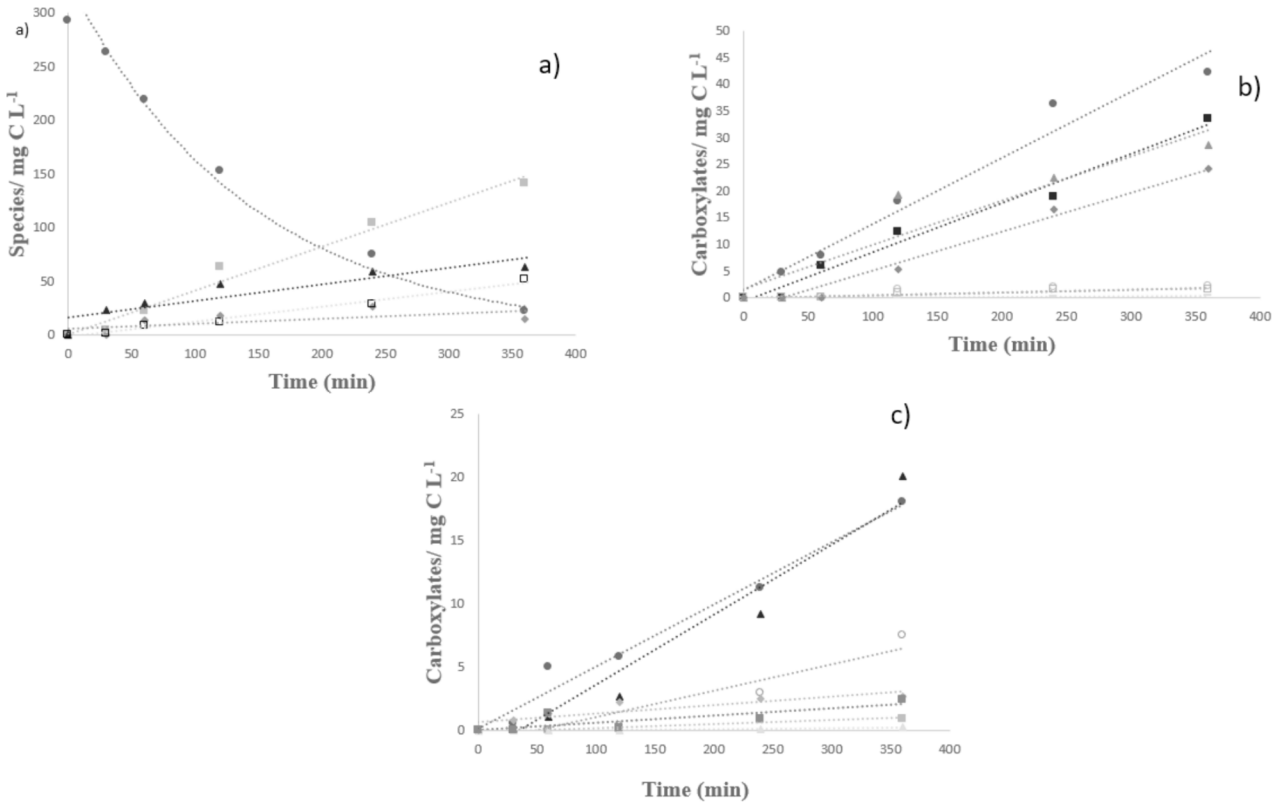

Fig. 8. Case study 2 in electro-refinery. Employing high current densities for both electrolysis (100 $mAcm^{-2}$ with an MMO anode) and electroseparation units (30 $mAcm^{-2}$ with an MMO anode). a) Illustrates species distribution during treatment: Phenol (●), carboxylates in tank 1 (■), carboxylates in tank 2 (□), Aromatics (◆), and CO_2 (▲). Graphics (b) and (c) detail the speciation of carboxylates in tanks 1 and 2, respectively, featuring Malonate (▲), Maleate (■), Acetate (◆), Oxalate (●), Succinate (▬), Oxamate (○), and Formate (□). The experimental wastewater contained 300 mg L^{-1} of phenol in a solution of 3.0 g/L NaOH and 3.0 g/L Na_2SO_4.

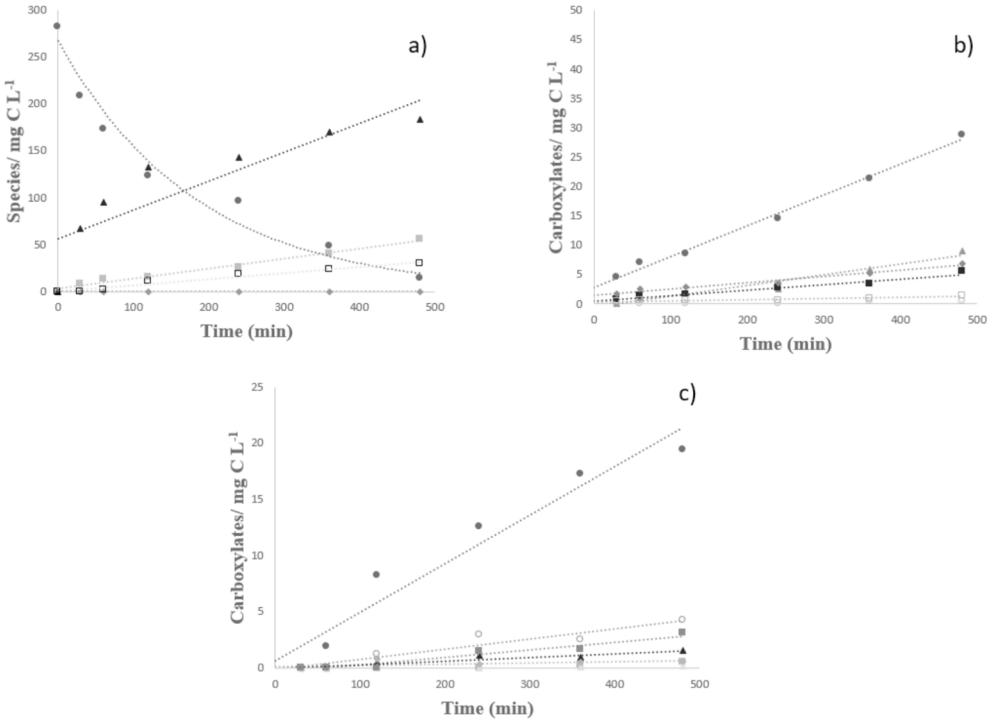

Fig. 9. Case study 3 in electro-refinery. Using high current densities for both electrolysis (100 mA cm^{-2} with a BDD anode) and electroseparation units (30 mA cm^{-2} with an MMO anode). a) Shows the overall species distribution during the process: Phenol (●), carboxylates in tank 1 (■), carboxylates in tank 2 (□), Aromatics (◆), and CO_2 (▲). Graphics (b) and (c) detail the carboxylate composition in tanks 1 and 2, respectively, featuring Malonate (▲), Maleate (■), Acetate (◆), Oxalate (●), Succinate (▬), Oxamate (○), and Formate (□). The wastewater tested had 300 mg L^{-1} of phenol in a solution of 3.0 g/L NaOH and 3.0 g/L Na_2SO_4.

of carboxylates generated during the electrolysis process are now being efficiently captured in the purified recovery solution within Tank 2.

Given the enhanced performance achieved by adjusting current densities, the potential for manipulating selectivity also deserves consideration. Beyond the choice of membranes, the composition of electrodes plays a crucial role in determining selectivity. Insights from section 2 highlighted that while a non-active anode like BDD may not be ideal for electroseparation, its distinct selectivity could offer advantages during the electrolysis phase. Therefore, an additional study was conducted to assess the impact of electrode material, wherein MMO anodes were substituted with a BDD anode in the electrolytic cell while maintaining the operational conditions from the previous experiment (100 mA cm^{-2} and 15 mA cm^{-2} for the electrolysis and electroseparation units, respectively).

The outcomes from this third case study, presented in Fig. 9, reveal that the harsher conditions induced by BDD electrodes do not favor the production of a broad range of carboxylates, with oxalate emerging as the predominant species. This result suggests a degree of selectivity, albeit with a significant increase in mineralization, which was observed to be threefold higher compared to the use of MMO electrodes. Such results underscore the superior suitability of MMO electrodes over BDD for this specific application.

Further analysis regarding the selection of anode materials, considering transport rates and efficiencies, is discussed in Fig. 10, demonstrating that the MMO anode is a superior option and that integrating the processes achieves greater transport rates and efficiencies compared to operating them separately.

In the integrated electro-refinery system, total transport rates of carboxylates across the membrane surface area achieved 138.7 mmol $m^{-2}h^{-1}$, surpassing the performance observed when the units were operated independently. The use of BDD anodes, while increasing mineralization, reduces transport efficiency to 71.6 mmol $m^{-2}h^{-1}$. Despite this, the composition of the carboxylate mixture shifts significantly with BDD usage, resulting in a solution where oxalate constitutes 75% of the mix, compared to only 48% when MMO anodes are employed.

Furthermore, the data also highlight the production efficiency, including the energy costs associated with the separation of carboxylates and the oxidation of synthetic waste in the electrolytic cell. The efficiency of carboxylate separation reaches 54.6 mmol kWh^{-1}, whereas the overall production efficiency stands at 8.77 mmol kWh^{-1}. The application of MMO anodes in the electrolytic unit enhances the overall production efficiency by nearly 50% compared to using BDD anodes, highlighting the advantages of MMO anodes in optimizing both the efficacy and the energy efficiency of the process.

To the author's knowledge, this integrated electro-refinery system is innovative and has not yet been reported in the literature. The application of such systems not only contributes to minimizing environmental impact, but also opens up new economic opportunities by transforming organic waste into value-added products, in line with the principles of sustainability and waste reduction [3,40].

4. Conclusions

This study introduces a transformative electrochemical approach for the production of high-value products from phenol, signifying a shift away from traditional wastewater treatment methods focused solely on mineralization. Demonstrating the effective electroproduction of carboxylic acids from contaminated wastewater, this research offers an advanced alternative to conventional (bio)refinery processes. It enables the repurposing of complex molecules found in wastewater, enhancing the value of the resulting treatment products. Through a systematic evaluation—initially analyzing components separately before integrating them into a cohesive process—this research establishes a novel treatment paradigm for the recovery of carboxylates derived from phenol degradation. Therefore, the most relevant conclusions drawn are:

- The integrated application of an electrolysis and electroseparation unit, as configured in this study, where the waste tank connects directly to both cells, facilitates the partial conversion of phenol in synthetic waste into carboxylates, followed by their recovery in a purified solution. This methodology exemplifies the potential for waste valorization by integrating the reactivity and separation

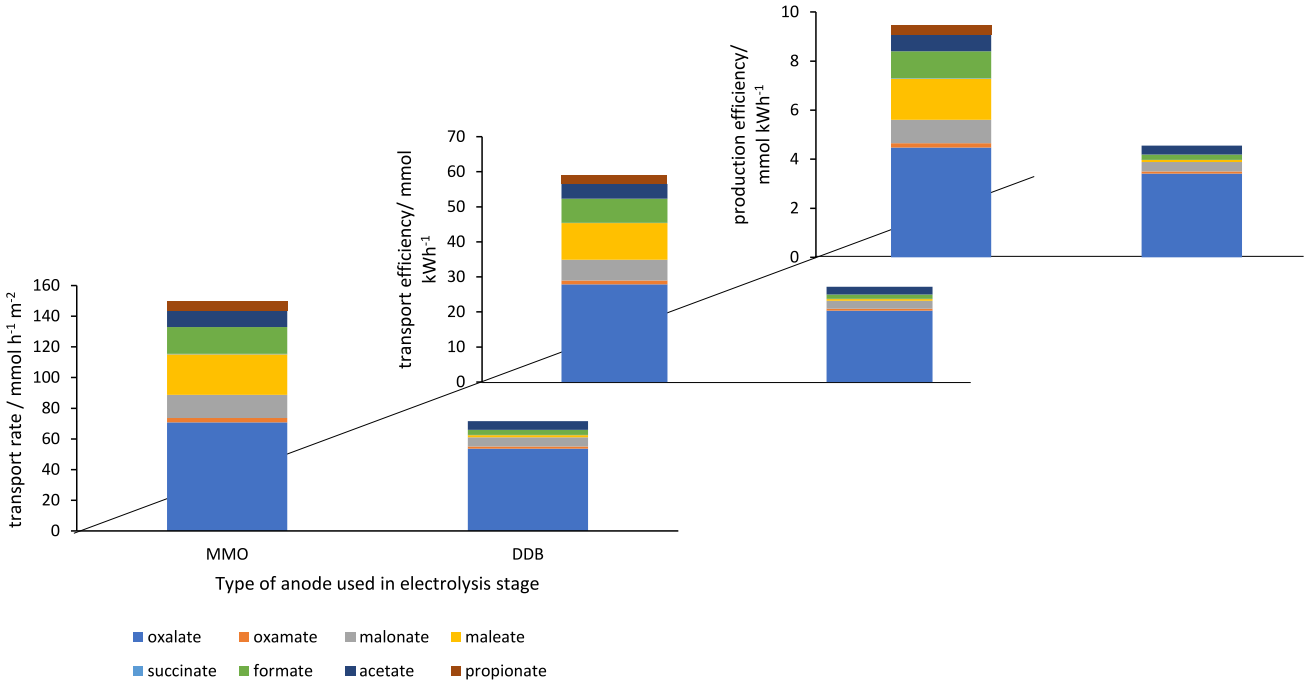

Fig. 10. Comparison of transport rate and efficiency between case studies 2 and 3. Case study 2 used an MMO anode, and case study 3 used a BDD anode. Both scenarios operated under conditions of 100 mA cm^{-2} for electrolysis and 30 mA cm^{-2} for electroseparation.

capacities of electrochemical technology into a novel paradigmatic concept.

- The choice of anode material and operational current densities emerge as critical factors in the electro-refinery framework, necessitating careful consideration in both the electrolytic and electroseparation processes. The selection of anode materials significantly affects reaction selectivity, with MMO anodes offering reduced mineralization compared to more aggressive alternatives such as BDD. While BDD anodes are not recommended for use in the electroseparation unit due to a lack of benefits, their selective impact on the carboxylate mixture composition may find utility in the electrolytic unit for specific applications. Notably, BDD anodes enhance the proportion of oxalates in the solution, demonstrating a 50% improvement in solution quality.
- Operational current density plays a vital role in modulating production rates, including formation and transport, as well as influencing mineralization rates. An optimal current density is, therefore, crucial. This study identifies 100 mA cm^{-2} in the electrolyzer and 30 mA cm^{-2} in the electroseparator as optimal values for utilizing MMO anodes.
- The integration of the treatment units yields superior results compared to their operation in sequence. The maximum carboxylate transport rates reached 138.7 mmol $m^{-2}h^{-1}$, with carboxylate separation efficiency from the reaction mixture as high as 54.6 mmol kWh^{-1}. Furthermore, the overall production efficiency was determined to be 8.77 mmol kWh^{-1}, highlighting the benefits of unit integration in enhancing process performance.

Declaration of competing interest

The authors declare that they have no known competing financial interests or personal relationships that could have appeared to influence the work reported in this paper.

Acknowledgments

This work is part of the research project PID2022-138401OB-I00 funded by MCIN/AEI/ and "Unión Europea Next Generation EU/PRTR. As well, this work is part of the research conducted within the E3tech+ network RED2022-134552-T, funded by MCIU/AEI/10.13039/501100011033. The authors acknowledge the funding received by the Brazilian funding agencies including the CNPq (grants: 200178/2022-9, 305438/2018-2, and 311856/2019-5), CAPES (grant: 88887.814609/2022-00) and FAPESP (grants: 2020/02743-4, 2022/03386-6, 2017/10118-0).

References

[1] S.Y. Pan, M.A. Du, I. Te Huang, I.H. Liu, E.E. Chang, P.C. Chiang, Strategies on implementation of waste-to-energy (WTE) supply chain for circular economy system: a review, J. Clean. Prod. 108 (2015) 409–421.
[2] A. Kumar, A.K. Thakur, G.K. Gaurav, J.J. Klemeš, V.K. Sandhwar, K.K. Pant, R. Kumar, A critical review on sustainable hazardous waste management strategies: a step towards a circular economy, Environ. Sci. Pollut. Res. 30 (2023) 105030–105055.
[3] S. Rezania, B. Oryani, V.R. Nasrollahi, N. Darajeh, M. Lotfi Ghahroud, K. Mehranzamir, Review on Waste-to-Energy Approaches toward a Circular Economy in Developed and Developing Countries, Processes 11 (2023).
[4] G. Venkatesh, Circular Bio-economy—Paradigm for the Future: Systematic Review of Scientific Journal Publications from 2015 to 2021, Circular Economy and Sustainability 2 (2022) 231–279.
[5] Z. Wysokińska, A review of transnational regulations in environmental protection and the circular economy, Comparative, Econ. Res. 23 (2020) 149–168.
[6] E.V. dos Santos, C.A. Martínez-Huitle, M.A. Rodrigo, The electro-refinery in organics: a new arising concept for valorization of wastes, Curr Opin, Electrochem (2023) 101267.
[7] H. Yu, I. Zahidi, C.M. Fai, D. Liang, D.Ø. Madsen, Mineral waste recycling, sustainable chemical engineering, and circular economy, Results in Engineering 21 (2024).
[8] C.A. Martínez-Huitle, M.A. Rodrigo, I. Sirés, O. Scialdone, A critical review on latest innovations and future challenges of electrochemical technology for the abatement of organics in water, Appl Catal B 328 (2023).
[9] C.A. Martínez-Huitle, I. Sirés, M.A. Rodrigo, Editorial overview: Electrochemical technologies for wastewater treatment with a bright future in the forthcoming years to benefit of our society, Curr. Opin. Electrochem. 30 (2021).
[10] B. Frontana Uribe, J. Solla Gullón, K. Bouzek, M. Andres Rodrigo, S. Garcia Segura's, V.J. Pais Vilar, D. Fatta Kassinos's, Electrochemistry in the water-energy-climate nexus, J. Environ. Chem. Eng. 11 (2023) 1–3.
[11] V. Kumar, S.A. Bhat, S. Kumar, P. Verma, I.A. Badruddin, J.H.P. Américo-Pinheiro, R. Sathyamurthy, A.E. Atabani, Tea byproducts biorefinery for bioenergy recovery and value-added products development: A step towards environmental sustainability, Fuel 350 (2023).
[12] J. Fehér, I. Červeňanský, L. Václavík, J. Markoš, Electrodialysis applied for phenylacetic acid separation from organic impurities: Increasing the recovery, Sep. Purif. Technol. 235 (2020).
[13] C. Huang, T. Xu, Y. Zhang, Y. Xue, G. Chen, Application of electrodialysis to the production of organic acids: State-of-the-art and recent developments, J Memb Sci 288 (2007) 1–12.
[14] P. Mandal, R. Mondal, P. Goel, E. Bhuvanesh, U. Chatterjee, S. Chattopadhyay, Selective recovery of carboxylic acid through PVDF blended anion exchange membranes using electrodialysis, Sep. Purif. Technol. 292 (2022).
[15] P.A. Hernandez, M. Zhou, I. Vassilev, S. Freguia, Y. Zhang, J. Keller, P. Ledezma, B. Virdis, Selective Extraction of Medium-Chain Carboxylic Acids by Electrodialysis and Phase Separation, ACS Omega 6 (2021) 7841–7850.
[16] G. Hopsort, Q. Cacciuttolo, D. Pasquier, Electrodialysis as a key operating unit in chemical processes: From lab to pilot scale of latest breakthroughs, Chem. Eng. J. 494 (2024).
[17] M.A. Alkhadra, X. Su, M.E. Suss, H. Tian, E.N. Guyes, A.N. Shocron, K.M. Conforti, J.P. De Souza, N. Kim, M. Tedesco, K. Khoiruddin, I.G. Wenten, J.G. Santiago, T. A. Hatton, M.Z. Bazant, Electrochemical Methods for Water Purification, Ion Separations, and Energy Conversion, Chem Rev 122 (2022) 13547–13635.
[18] C.H. Comninellis, C. Pulgarin, Anodic oxidation of phenol for waste water treatment, 1991.
[19] C. Comninellis, A. Nerini, Anodic oxidation of phenol in the presence of NaCI for wastewater treatment, 1995.
[20] C. Comninellis, C. Pulgarin, Electrochemical oxidation of phenol for wastewater treatment using SnO2 anodes, 1993.
[21] P. Cañizares, J.A. Domínguez, M.A. Rodrigo, J. Villaseñor, J. Rodríguez, Effect of the current intensity in the electrochemical oxidation of aqueous phenol wastes at an activated carbon and steel anode, Ind. Eng. Chem. Res. 38 (1999) 3779–3785.
[22] P. Cañizares, M. Díaz, J.A. Domínguez, J. García-Gómez, M.A. Rodrigo, Electrochemical oxidation of aqueous phenol wastes on synthetic diamond thin-film electrodes, Ind. Eng. Chem. Res. 41 (2002) 4187–4194.
[23] P. Cañizares, F. Martínez, M. Díaz, J. García-Gómez, M.A. Rodrigo, Electrochemical Oxidation of Aqueous Phenol Wastes Using Active and Nonactive Electrodes, J. Electrochem. Soc. 149 (2002) D118.
[24] R.S. de S. Castro, A.R. Dória, F. Costa, S. Mattedi, K.I.B. Eguiluz, G.R. Salazar-Banda, Dipropyl ammonium ionic liquids to prepare Ti/RuO_2–Sb_2O_4 anodes at different calcination temperatures, Environmental Science and Pollution Research (2023).
[25] L.M. da Silva, I.F. Mena, M.A. Montiel, C. Saez, A.J. Motheo, M.A. Rodrigo, Electrochemical generation of ozone for application in environmental remediation, Results in Engineering 20 (2023).
[26] D.Y. López-Chico, H. Pérez-Vidal, G. Torres, M.A. Lunagómez, B. Pawelec, R. M. Navarro Yerga, P.J. Vázquez-Salas, T.A. Zepeda, Improved phenol degradation by catalytic wet air oxidation on the Co_3O_4 spinel catalysts supported on SBA-15 modified with TiO2, J. Catal. 429 (2024).
[27] H. Ma, X. Zhang, Q. Ma, B. Wang, Electrochemical catalytic treatment of phenol wastewater, J. Hazard. Mater. 165 (2009) 475–480.
[28] Y. Dehmani, D. Dridi, T. Lamhasni, S. Abouarnadasse, R. Chtourou, E.C. Lima, Review of phenol adsorption on transition metal oxides and other adsorbents, J. Water Process Eng. 49 (2022).
[29] G. Hurwitz, P. Pornwongthong, S. Mahendra, E.M.V. Hoek, Degradation of phenol by synergistic chlorine-enhanced photo-assisted electrochemical oxidation, Chem. Eng. J. 240 (2014) 235–243.
[30] R. Berenguer, J.M. Sieben, C. Quijada, E. Morallón, Electrocatalytic degradation of phenol on Pt- and Ru-doped Ti/SnO_2-Sb anodes in an alkaline medium, Appl Catal B 199 (2016) 394–404.
[31] S.N. Hussain, H.M.A. Asghar, A.K. Campen, N.W. Brown, E.P.L. Roberts, Breakdown products formed due to oxidation of adsorbed phenol by electrochemical regeneration of a graphite adsorbent, Electrochim. Acta 110 (2013) 550–559.
[32] X. Duan, F. Ma, Z. Yuan, X. Jin, L. Chang, Electrochemical degradation of phenol in aqueous solution using PbO2 anode, J. Taiwan Inst. Chem. Eng. 44 (2013) 95–102.
[33] M.C. Medeiros, S.S.L. Castro, E.V. dos Santos, M.A. Rodrigo, C.A. Martínez-Huitle, A proof of concept for the electro-refinery: Selective electroproduction of acetic acid from t-CNSL waste by using DSA electrode, Electrochem. Commun. 141 (2022).
[34] A. Phetrak, P. Westerhoff, S. Garcia-Segura, Low energy electrochemical oxidation efficiently oxidizes a common textile dye used in Thailand, J. Electroanal. Chem. 871 (2020).
[35] E.M.S. Oliveira, F.R. Silva, C.C.O. Morais, T.M.B.F. Oliveira, C.A. Martínez-Huitle, A.J. Motheo, C.C. Albuquerque, S.S.L. Castro, Performance of (in)active anodic materials for the electrooxidation of phenolic wastewaters from cashew-nut processing industry, Chemosphere 201 (2018) 740–748.

[36] M.C. Medeiros, J.B. de Medeiros, C.A. Martínez-Huitle, T.M.B.F. Oliveira, S. E. Mazzetto, F.F.M. da Silva, S.S.L. Castro, Long-chain phenols oxidation using a flow electrochemical reactor assembled with a TiO_2-RuO_2-IrO_2 DSA electrode, Sep. Purif. Technol. 264 (2021) 118425.
[37] M.C. Medeiros, E.V. dos Santos, C.A. Martínez-Huitle, A.S. Fajardo, S.S.L. Castro, Obtaining high-added value products from the technical cashew-nut shell liquid using electrochemical oxidation with BDD anodes, Sep. Purif. Technol. 250 (2020).
[38] Y. Yu, H. Jin, Q. Li, X. Zhang, Y. Zhang, X. Chen, Pseudocapacitive Ti/RuO_2-IrO_2-RhOx electrodes with high bipolar stability for phenol degradation, Sep. Purif. Technol. 263 (2021).
[39] S.O. Ganiyu, N. Oturan, C. Trellu, S. Raffy, M. Cretin, C. Causserand, M.A. Oturan, Abatement of analgesic antipyretic 4-aminophenazone using conductive boron-doped diamond and sub-stoichiometric titanium oxide anodes: Kinetics, mineralization and toxicity assessment, ChemElectroChem 6 (2019) 1808–1817.
[40] Y. Duan, A. Tarafdar, V. Kumar, P. Ganeshan, K. Rajendran, B. Shekhar Giri, R. Gómez-García, H. Li, Z. Zhang, R. Sindhu, P. Binod, A. Pandey, M.J. Taherzadeh, S. Sarsaiya, A. Jain, M. Kumar Awasthi, Sustainable biorefinery approaches towards circular economy for conversion of biowaste to value added materials and future perspectives, Fuel 325 (2022).